Journal of Geodynamics 56–57 (2012) 76–85

Contents lists available at SciVerse ScienceDirect

Journal of Geodynamics

journal homepage: http://www.elsevier.com/locate/jog

Evidence for ~80–75 Ma subduction jump during Anatolide–Tauride–Armenian block accretion and ~48 Ma Arabia–Eurasia collision in Lesser Caucasus–East Anatolia

Yann Rolland[a,*], Dogan Perincek[b], Nuretdin Kaymakci[c], Marc Sosson[a], Eric Barrier[d], Ara Avagyan[e]

[a] Géoazur, Université de Nice Sophia Antipolis, Observatoire de la Côte d'Azur, Facultés des Sciences, Parc Valrose, Nice, France
[b] Canakkale Onsekiz Mart University, Faculty of Engineering and Architecture, Department of Geological Engineering, Terzioglu Campus 17020 Canakkale, Turkey
[c] Remote Sensing and GIS Laboratory, Department of Geological Engineering, Middle East Technical University, 06531 Ankara, Turkey
[d] Université Pierre et Marie Curie - Paris VI, Laboratoire de Tectonique - CNRS UMR 7072, 4 Place Jussieu F-75252 Paris Cedex 05 France, France
[e] Institute of Geological Sciences, National Academy of Sciences of Armenia, 24a Baghramian Avenue, Yerevan 375019, Armenia

ARTICLE INFO

Article history:
Received 17 January 2011
Received in revised form 12 August 2011
Accepted 29 August 2011
Available online 10 September 2011

Keywords:
$^{40}Ar/^{39}Ar$ dating
Neotethys
Lesser Caucasus
Obduction
Accretion

ABSTRACT

Orogens formed by a combination of subduction and accretion are featured by a short-lived collisional history. They preserve crustal geometries acquired prior to the collisional event. These geometries comprise obducted oceanic crust sequences that may propagate somewhat far away from the suture zone, preserved accretionary prism and subduction channel at the interplate boundary. The cessation of deformation is ascribed to rapid jump of the subduction zone at the passive margin rim of the opposite side of the accreted block. Geological investigation and $^{40}Ar/^{39}Ar$ dating on the main tectonic boundaries of the Anatolide–Tauride–Armenian (ATA) block in Eastern Turkey, Armenia and Georgia provide temporal constraints of subduction and accretion on both sides of this small continental block, and final collisional history of Eurasian and Arabian plates. On the northern side, $^{40}Ar/^{39}Ar$ ages give insights for the subduction and collage from the Middle to Upper Cretaceous (95–80 Ma). To the south, younger magmatic and metamorphic ages exhibit subduction of Neotethys and accretion of the Bitlis–Pütürge block during the Upper Cretaceous (74–71 Ma). These data are interpreted as a subduction jump from the northern to the southern boundary of the ATA continental block at 80–75 Ma. Similar back-arc type geochemistry of obducted ophiolites in the two subduction–accretion domains point to a similar intra-oceanic evolution prior to accretion, featured by slab steepening and roll-back as for the current Mediterranean domain. Final closure of Neotethys and initiation of collision with Arabian Plate occurred in the Middle-Upper Eocene as featured by the development of a Himalayan-type thrust sheet exhuming amphibolite facies rocks in its hanging-wall at c. 48 Ma.

1. Introduction

The structures of orogens resulting from the accretion (or 'collage') of small continental blocks are most often obliterated in the following collisional history of larger continental blocks, which will eventually transpose the accretion belt (e.g., Vanderhaeghe, 2012; Rolland et al., 2012). In this concern, the Eastern Anatolia–Lesser Caucasus tectonic domain provides a rare example of preserved geometries formed by subduction of oceanic domains and subduction–accretion of continental blocks. The history of this large tectonic belt is still largely unconstrained because of the lack of key geochronological data on the main suture zones. In particular, the timing of block accretions and along-belt lateral correlations remain the focus of ongoing research. We present here a synthesis of recent data acquired on the Georgia–Armenia–Eastern Turkey transect, along with some unpublished petrologic and $^{40}Ar/^{39}Ar$ geochronological data. These data allow integrating the accretion history of blocks between the Georgian Eurasian margin and Arabian, along a N–S transect from the Lesser Caucasus in the north to the Taurides in the South, on both sides of the so-called 'Anatolide–Tauride–Armenian' (ATA) continental block.

2. Geological setting

For the detailed geology we refer to papers by Galoyan et al. (2009), Sosson et al. (2010), and Rolland et al. (2009a,b, 2010, 2011) for the geology of the northern (Armenia–Georgia–Azerbaijan) part and to Perinçek and Özkaya (1981), Kaymakci et al. (2009, 2010) and Yılmaz (1993) for the southern Turkish part of the transect. Main

* Corresponding author.
E-mail addresses: yrolland@unice.fr, Yann.Rolland@unice.fr (Y. Rolland).

0264-3707/$ – see front matter © 2011 Elsevier Ltd. All rights reserved.
doi:10.1016/j.jog.2011.08.006

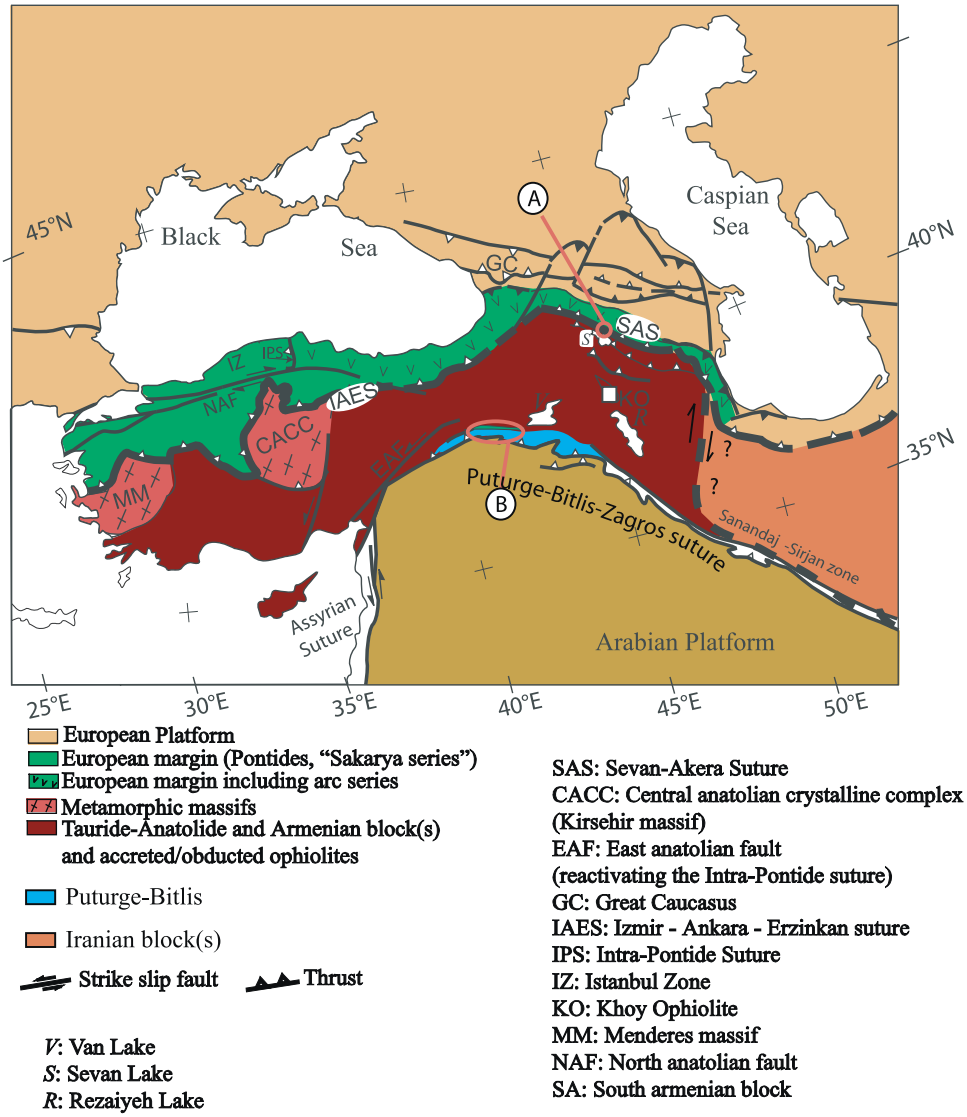

Fig. 1. Sketch of geological map of the Caucasus region, showing the locations of A, North Armenian flysch and B, Enlarged map of SE Turkey shown on Fig. 7.

geological features of the Lesser Caucasus are summarized below from north to south.

2.1. Main tectonic sutures

Two main suture zones are defined along strike of the Turkish-Armenian collision zone (Figs. 1 and 2):

(1) The Izmir–Ankara–Erzincan suture in Turkey, with its eastern extension in Northern Armenia, the Amassia–Sevan suture, which separates the ATA continental block(s) from the Eurasian margin to the North in Georgia. This suture records formation of Neotethyan back-arc oceanic crust in the Middle-Upper Jurassic (Galoyan et al., 2007, 2009; Rolland et al., 2009a, 2010, 2011). Subduction of the oceanic domain separating the ATA block from the Eurasian margin ended in the early Upper Cretaceous.

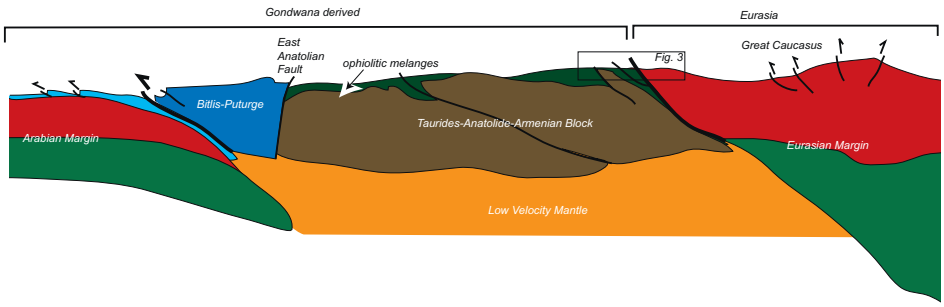

Fig. 2. Crustal-scale cross-section of the Great Caucasus–Arabia transect, modified after Sosson et al. (2010).

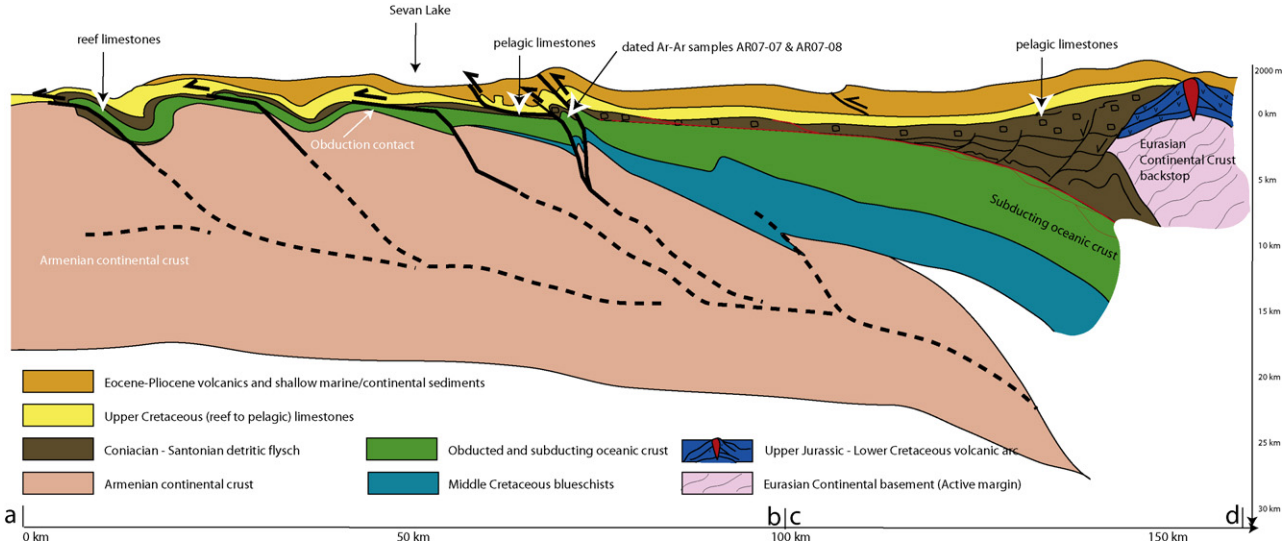

Fig. 3. Interpretative crustal-scale sketch cross-section of the SE Turkey–Georgian transect (see position on Fig. 2).

Blueschists dated at 100–90 Ma are recorded in both NW Turkey (Okay et al., 2006) and North Armenia (Rolland et al., 2009a). Obduction of the Armenian ophiolites onto the ATA block(s) occurred in the Coniacian-Santonian (c. 85 Ma; Sosson et al., 2010) prior to suturing in the Upper Cretaceous-Lower Paleocene (71–73 Ma, Rolland et al., 2009a, 2011).

(2) To the south, the main suture separating the ATA block(s) from the Arabian plate is the Pütürge–Bitlis–Zagros suture zone, which witnessesed northward subduction of Neo-Tethys below the Iranian and ATA active margins (e.g., Agard et al., 2005 and references therein; Figs. 1 and 2). Ophiolitic rocks are found both sides of the Pütürge–Bitlis continental massif (Fig. 4), indicating that the Bitlis has been a separate crustal block (Oberhänsli et al., 2010). Further east in Oman, obduction of the Semaï ophiolite onto the Arabian margin occurred at c. 85 Ma (Ricou et al., 1986). Later on, continental subduction of the Bitlis–Pütürge Massif below the ATA block(s) is documented by white mica Ar–Ar age of 74 ± 2 Ma (Oberhänsli et al., 2010), supported by white mica and whole rock K–Ar ages of ~74–71 Ma (Göncüoğlu and Turhan, 1984; Hempton, 1985). Uplift and final exhumation of the Bitlis range ($T < 120\,^{\circ}C$) by 18–13 Ma is documented on the basis of apatite fission track dating (Okay et al., 2010). Further collision of the Arabian margin below the Bitlis–Pütürge is still debated but has been proposed as Late Eocene–Oligocene on the basis of structural and stratigraphic data (Fig. 4). Hempton (1985) proposed a mid to late Eocene age, while Yılmaz (1993) proposed a Late Eocene to Oligocene age and finally Robertson postulated a post-Eocene (probably Oligocene) age for closure of the southern branch of Neotethys. Molassic sedimentary markers of continental uplift are identified since the Lower Oligocene (Hüsing et al., 2009 and references therein). Uplift rapidly transferred into the whole Lesser Caucasus belt and reached the Great Caucasus in the earliest Oligocene (Vincent et al., 2005). Accordingly, in the Zagros, Agard et al. (2005) suggest collision shortly after 35 Ma prior to late Oligocene sedimentation.

2.2. Obducted ophiolite sequences

The Lesser Caucasus orogen preserves an obducted ophiolite sequence, outcropping along the NE Turkey, Armenia and SW Arzerbaijan areas (Figs. 1 and 2). Lordkipanidze et al. (1989) first suggested a Middle Jurassic 'Mariana-type' subduction in this (Lesser Caucasus) region. The oceanic crust lithologies within the ophiolite nappe are Late Jurassic in age (170–160 Ma; Danelian et al., 2008; Galoyan et al., 2009; Rolland et al., 2009b, 2010). They have a geochemical composition intermediate between MORB and arc series, while being emplaced in deep marine slow-spreading basins. These features are interpreted as representative of an intra-oceanic back-arc basin. The ophiolites were obducted to the south over the Tauride–Anatolian–Armenian block(s) (Figs. 2 and 3) during the Coniacian-Santonian times (~85 Ma; see previous paragraph). Some blueschist facies metamorphic rocks are found in tectonic windows, and are structurally below the ophiolite with HP-LT stage at 94–90 Ma followed by a retrograde Green Schist/Epidote Amphibolite metamorphism (~500 °C) during exhumation in the Late Cretaceous at 71–74 Ma (Rolland et al., 2009a). Arc-related volcanic rocks found on top of the ophiolite and HP rocks evidence N-dipping subduction, which was active before the continental block underthrusting below the ophiolite (Galoyan et al., 2007, 2009; Rolland et al., 2009a). In the same time, the northern margin of the remaining oceanic domain was still subducting below Eurasia, leading to a very thick Andean margin built onto the Georgian continental basement in the Jurassic and Lower Cretaceous (Adamia et al., 1981; Rolland et al., 2011). Following the phase of continental subduction or ophiolite obduction, the ophiolite was partly eroded and overlain by conglomerates and some platform-type carbonates. The remaining basin closure occurred shortly after, by the entry of the South-Armenian block and obducted ophiolite into the north subduction system. Due to the blocking of the northern subduction zone, a new subduction zone was rapidly activated to the south of the ATA block(s). This more southerly subduction is shown by blueschists of the Bitlis massif (SE Turkey) dated at 74 ± 2 Ma (Oberhänsli et al., 2010). Therefore, due to the stopping of subduction motions on the northern rim of the ATA block(s), the overall geometry preserved in NE Armenia–Karabakh region is that of an active margin similar to the current situation of the Andes (Rolland et al., 2011). Preliminar geological investigations allow the reconstruction of a geological section showing the oceanic crust-accretionary prism contact preserved (Fig. 3). Only very slight Cenozoic deformation has occurred along the Sevan–Akera suture zone, which is partly reactivated along the northern side of Sevan Lake (Galoyan et al., 2009). In the Karabakh region, this late

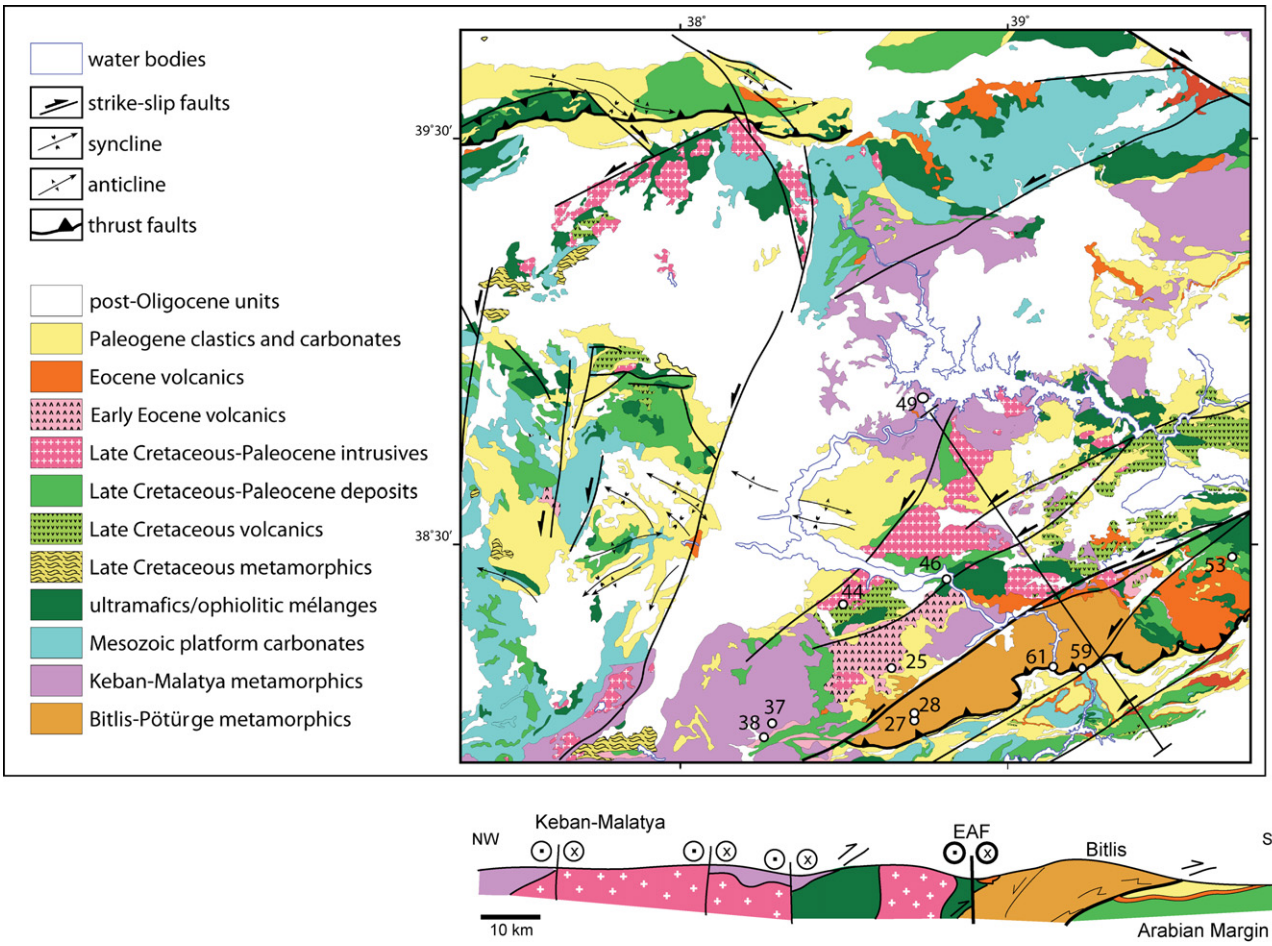

Fig. 4. Sketch of geological map and geological cross-section of SE Turkey Taurides–Anatolides belt, with locations of analysed samples. EAF, East Anatolian Fault.

reactivation is shown by large wave-length folds and some discrete faults.

3. Geochemistry of SE Turkey obducted ophiolite sequences

Three representative samples of the Maden volcanic unit, which comprises ophiolitic material outcropping to the north of the Bitlis–Pütürge massif (Fig. 4) are used to infer the geodynamic setting of this oceanic segment. Analyses were undertaken at the CRPG (Nancy), details on procedures can be seen on http://helium.crpg-nancy.fr/SARM. Results are summarized in Table 1 and Fig. 5. The three samples are of andesitic (Loc44), basaltic (Loc46), andesitic basalt (Loc53) compositions, respectively considering their major element composition. Trace element contents show a calc-alkaline (Loc44) to tholeiitic (Loc46) volcanic arc affinity, supported by Nb–Ta and Ti depletions on MORB-normalized plots. The gabbro sample (Loc46) has a composition similar to those of back-arc basalts (Cabanis and Lecolle, 1989) with a strong tholeiitic composition and a slight subduction component. The three samples are therefore indicative of an immature to mature arc system, emplaced between the ATA and Arabian margins, thrusted over the Bitlis–Pütürge continental unit. These data agree with petro-geochemical data of Late Cretaceous ophiolites to the South of Taurides in Turkey, Troodos in Cyprus and Baer-Bassit in Syria. It is widely known at a regional scale that these ophiolites formed in a supra-subduction zone environment (e.g., Lytwyn and Casey, 1993; Yalınız et al., 1996; Floyd et al., 2000; Parlak et al., 1996, 2000, 2009; Robertson, 2002; Kuscu et al., 2010) (Tables 2 and 3).

4. $^{40}Ar/^{39}Ar$ dating

4.1. Analytical techniques

White micas and amphiboles were analysed by electron microprobe (EPM) analysis to check whether the mineral compositions are homogeneous from core to rim. EPM analysis was done in Blaise Pascal University (Clermont-Ferrand) with a Cameca SX100 electron microprobe in Clermont Ferrand University, using a 15 kV and 1 nA beam current, with natural samples as standards. Grains less than 500 μm were separated by careful selection by hand-picking under a binocular microscope, to prevent the presence of altered grains. Analyses of the single grains of amphibole and white mica of 250–500 μm size (~0.2 mg) were undertaken by step heating with a 50 W CO_2 Synrad 48-5 continuous laser beam. Measurement of isotopic ratios was done with a VG3600 mass spectrometer, equipped with a Daly detector system; we refer to Jourdan et al. (2006) for details of the procedure. Summary of results are presented in Table 1 and Figs. 4 and 5, and are discussed below.

4.2. Dating of the Keban-Malatya metamorphic complex

The Keban-Malatya metamorphic complex comprises high-temperature metamorphosed fluorite-bearing white marble layers (sample Loc49, Fig. 6C), which provided a Muscovite age of 73.8 ± 0.3 Ma (Fig. 7A). This metamorphism is related to a high geothermal gradient related to supra-subduction magmatism in the ATA block(s) during the Campanian.

Table 1
Geochemical data of magmatic rocks from Maden Unit (SE Turkey).

Sample no	LOC44	LOC46	LOC53
Rock type	Andesite	Gabbro	Basalt
SiO_2 (%)	59.26	46.90	50.93
TiO_2 (%)	0.71	1.12	1.83
Al_2O_3 (%)	13.65	17.02	15.49
Fe_2O_3 (%)	8.06	11.06	12.02
FeO (%)			
MnO (%)	0.14	0.24	0.14
MgO (%)	4.14	7.16	5.16
CaO (%)	7.42	10.67	4.17
Na_2O (%)	2.06	2.73	4.42
K_2O (%)	0.33	0.62	0.54
P_2O_5 (%)	0.08	0.21	0.45
LOI (%)	3.83	1.96	3.70
H_2O			
Total (%)	99.68	99.69	98.85
Ba (ppm)	32	168	35
Rb (ppm)	6.0	9.1	11.2
Sr (ppm)	127	314	156
Ta (ppm)	0.05	0.16	0.66
Th (ppm)	0.34	0.67	1.26
Zr (ppm)	64	49	310
Nb (ppm)	0.6	2.6	8.2
Y (ppm)	25.60	25.90	92.10
Hf (ppm)	1.99	1.59	8.20
V (ppm)	223	348	123
Cr (ppm)	86	110	8
Ni (ppm)	29.1	36.4	10.1
Co (ppm)	22	35	18
U (ppm)	0.21	0.18	0.33
Cu (ppm)	44	56	24
Zn (ppm)	73	101	136
Pb (ppm)	2.03	2.22	2.27
Cs (ppm)	0.14	3.22	0.32
La (ppm)	3.1	11.3	13.7
Ce (ppm)	7.9	24.7	36.2
Pr (ppm)	1.23	3.30	5.42
Nd (ppm)	7.6	17.0	31.1
Sm (ppm)	2.61	4.18	9.74
Eu (ppm)	0.79	1.41	2.96
Gd (ppm)	3.39	4.23	11.90
Tb (ppm)	0.60	0.69	2.15
Dy (ppm)	4.10	4.33	14.60
Ho (ppm)	0.89	0.89	3.22
Er (ppm)	2.67	2.58	9.56
Tm (ppm)	0.41	0.40	1.47
Yb (ppm)	2.89	2.79	10.10
Lu (ppm)	0.46	0.43	1.56

4.3. Dating of the Maden magmatic unit

South of the Malatya metamorphic complex, at the base of Maden magmatic unit, the gabbro sample (Loc46, Fig. 6D) comprising back-arc geochemical signature (discussed in Section 3) provided an unexpected young age of c. 80 Ma. Two amphibole single-grain dating experiments (K138 and K123) provided 78.7 ± 1.0 Ma and 81.9 ± 0.6 Ma, respectively (Fig. 7B and C). The slight difference in age of the two experiments is ascribed to mineral crystallization discrepancies, as amphibole crystallized during possibly long hydrothermal process (e.g., Rolland et al., 2009c). These geochemical and geochronological data are interpreted as the indication of a syn-convergence arc-related basin in the Lower Campanian, which likely closed in the Upper Campanian.

4.4. Dating of the Pütürge metamorphic unit

South of this oceanic suture, Pütürge micaschists (Loc28, Fig. 6E and F) exhibit an Upper Campanian age of 70.7 ± 0.3 Ma on phengite (Fig. 7D), which indicates that HP metamorphism, and thus subduction of the Pütürge unit below the Malatya complex, occurred at this time. This age is similar to that of HP metamorphism in the Bitlis unit (Oberhänsli et al., 2010). This data evidence that Pütürge and Bitlis units underwent a similar tectonic history.

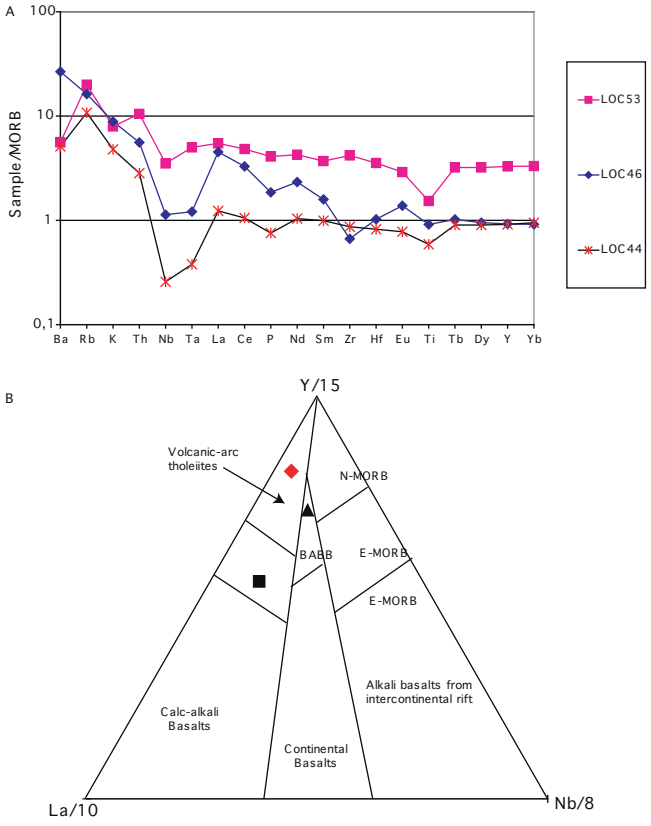

Fig. 5. Geochemical features of Maden magmatic rocks, including Late Cretaceous volcanics (location 44 in Fig. 4), gabbro (location 46 in Fig. 4) and basalt (location 53 in Fig. 4) from the ophiolitic sole. A, MORB-Normalized plots and B, Cabanis and Lecolle (1989) diagram.

4.5. Dating of the basal shear zone of Pütürge metamorphic unit

At the base of the Pütürge unit, amphibolites were sampled along a broad top-to-the South shear zone (Loc 59, Fig. 6G–I). Thermobarometry performed on sample Loc 59 yields *P–T* estimates of 6.0 ± 0.5 kbar and 550 ± 25 °C (Fig. 8). *P–T* data agree for burial of metabasalt/metagabbro lithologies tightly folded with metasediments, within a hot geothermal gradient of ~23 °C km^{-1}. These rocks exhibit much younger ages than for the rest of the section. Ar–Ar dating yielded an age of 48.0 ± 0.8 Ma (Fig. 7E). In our interpretation, the amphibolites likely provide the time for the tectonic transport of the Pütürge onto the Arabian margin, featured by top-to-south sense of shear marked by the metamorphic minerals (Fig. 6H), and thus exhumation of the Pütürge-Malatya units, in the Lutetian (Eocene) times.

5. Discussion

In the following, we propose a synthesis for the timing of geodynamic events in the formation of the Caucasus orogen. The sequence of events is regarded as a succession of accretions following a short continental subduction period, resulting in a 'growing southward' Eurasian margin. The dating of main Lesser Caucasus–East Anatolia suture zones are integrated into a sketch evolutionary model (Fig. 9), which is discussed below.

Table 2
Summary of $^{40}Ar/^{39}Ar$ dating results from Lesser Caucasus magmatic and metamorphic rocks.

Sample noStep no	Laser power (mW)	Atmospheric content (%)	^{39}Ar (%)	$^{37}Ar_{Ca}/^{39}Ar_K$	$^{40}Ar^*/^{39}Ar_K$ (±1 s)	Age (Ma ± 1 s)
K121-**Loc49** Muscovite/J: 0.0034/plateau age: 73.8 ± 0.3 Ma (2 s-100% ^{39}Ar)/inverse isochron age: 73.0 ± 0.5 Ma (2 s-100% ^{39}Ar, MSWD: 2.08)						
1	442	8.77	4.3	–	12.49 ± 0.12	75.4 ± 0.7
2	483	4.16	12.2	–	12.28 ± 0.05	74.2 ± 0.3
3	503	2.29	12.1	0.15	12.36 ± 0.06	74.7 ± 0.4
4	515	0.00	3.1	–	12.40 ± 0.15	74.9 ± 0.9
5	3333	2.07	68.3	–	12.16 ± 0.04	73.5 ± 0.2
K123-**Loc46** Amphibole/J: 0.0034/plateau age: 81.9 ± 0.6 Ma (2 s-99% ^{39}Ar)/inverse isochron age: 79.9 ± 0.4 Ma (2 s-100% ^{39}Ar, MSWD: 1.16)						
1	422	77.93	0.9	39.80	55.69 ± 3.89	315 ± 20
2	450	18.48	5.4	9.81	13.39 ± 0.28	80.9 ± 1.6
3	636	8.10	33.1	7.00	13.60 ± 0.08	82.1 ± 0.5
4	706	5.22	26.6	6.28	13.47 ± 0.08	81.4 ± 0.5
5	1200	7.99	34.1	7.73	13.62 ± 0.08	82.2 ± 0.5
K137-**Loc28** phengite/J: 0.0035/plateau age: 70.7 ± 0.3 Ma (2 s-89% ^{39}Ar)/inverse isochron age: 77.5 ± 0.7 Ma (2 s-89% ^{39}Ar, MSWD: 0.12)						
1	446	11.79	11.0	1.23	10.79	66.0 ± 0.6
2	557	0.31	52.4	0.01	11.56	70.7 ± 0.2
3	574	–	7.5	0.01	11.54	70.5 ± 0.6
4	593	–	13.0	–	11.58	70.8 ± 0.3
5	607	–	5.8	–	11.58	70.8 ± 0.4
6	620	–	3.1	0.03	11.62	71.0 ± 1.5
7	1888	–	7.1	0.29	11.75	71.8 ± 0.5
K138-**Loc46** Amphibole (duplicate)/J: 0.0229/plateau age: 78.7 ± 1.0 Ma (2 s-97.0% ^{39}Ar)/inverse isochron age: 77.5 ± 0.7 Ma (2 s-97% ^{39}Ar, MSWD: 0.3)						
1	464	80.71	1.0	15.04	8.43 ± 0.64	318 ± 22
2	494	92.31	0.4	4.90	0.21 ± 0.67	9 ± 28
3	543	46.88	1.5	5.31	1.16 ± 0.11	47.3 ± 4.5
4	626	18.28	25.4	6.13	1.93 ± 0.02	77.7 ± 0.9
5	670	11.63	49.9	5.45	1.96 ± 0.02	79.2 ± 0.7
6	700	7.88	2.7	6.16	1.97 ± 0.16	79.3 ± 6.1
7	1111	8.23	19.1	6.26	1.95 ± 0.02	78.7 ± 0.8
K139-**Loc59** Amphibole/J: 0.0229/plateau age: 48.0 ± 0.8 Ma (2 s-91.4% ^{39}Ar)/inverse isochron age: 47.1 ± 1.2 Ma (2 s-100% ^{39}Ar, MSWD: 0.6)						
1	458	63.77	1.8	2.63	1.67 ± 0.48	67 ± 19
2	509	55.50	2.6	2.52	1.24 ± 0.27	50 ± 11
3	558	24.14	3.2	5.26	1.03 ± 0.12	42.1 ± 5.0
4	642	28.23	42.4	10.47	1.16 ± 0.03	47.3 ± 1.2
5	697	15.37	41.1	10.78	1.19 ± 0.02	48.3 ± 0.9
6	726	2.75	2.1	9.27	1.21 ± 0.19	49.2 ± 7.7
7	1888	7.29	6.8	10.39	1.23 ± 0.15	50.1 ± 5.3
K201-**AR0709** Amphibole/J: 0.0182/plateau age: 166.3 ± 1.8 Ma (2 s-57% ^{39}Ar)/inverse isochron age: 166.8 ± 0.5 Ma (2 s-100% ^{39}Ar, MSWD: 0.2)						
1	400	99.0	1.3	5.36	1.35	44 ± 44
2	453	87.4	2.7	16.21	4.50	142 ± 18
3	524	50.7	21.7	103.11	4.71	148.1 ± 2.1
4	559	17.2	17.6	173.63	5.10	159.9 ± 1.4
5	593	15.8	24.0	269.63	5.29	165.6 ± 1.7
6	625	4.5	11.3	315.00	5.36	167.7 ± 1.8
7	1111	3.7	21.2	399.83	5.32	166.4 ± 1.1

5.1. The North Armenian flysch: evidence for Armenian block accretion to Eurasian Margin in the Coniacian-Santonian times

The North Armenian flysch unconformably overlies the Sevan–Akera ophiolite. It is Coniacian-Santonian in age and seals the suture zone (Sosson et al., 2010). The flysch structural position is in front of a north-dipping subduction zone below the Eurasian active margin of Georgia (Fig. 3). This time range is slightly younger (by several Ma) to that of ophiolite obduction onto the ATA block(s). Rolland et al. (2011) reported Ar–Ar amphibole and mica ages of ~166–167 Ma in a ~10 m large block sampled within the N-Armenian flysch, directly south of the Eurasian margin suture zone (Fig. 6A and B). The metamorphic ages of the exotic block are in agreement with provenance from the Georgian Eurasian basement to the north. Although these exotic blocks could have been transported as turbiditic flows along a steep margin, the Eurasian margin was then already lying just north of the Armenian block. Then this is clear that the back-arc basin separating the Armenian block from the Eurasian margin was consequently closed at that time.

5.2. Subduction jump in the Campanian times (75–80 Ma)

Until the Campanian most of the oceanic space between the Eurasian and Arabian plates was absorbed by subduction below an intra-oceanic arc/back-arc system and along the Georgian active margin, in a way similar as the current SW Pacific situation (Galoyan et al., 2009; Rolland et al., 2009a). The main geodynamic events that occurred between the Eurasian and ATA block(s) margins are (1) formation of a slow-spreading back-arc oceanic crust in the

Table 3
GPS coordinates (WGS grid) and geological units of analysed samples (SE Turkey).

Loc28	Pütürge metamorphics	38°6′9.80″N	38°44′18.10″E
Loc44	Yuksekova-Campanian	38°19′53.20″N	38°30′38.90″E
Loc46	Komurhan ophiolite Yuksekova	38°26′25.50″N	38°49′28.60″E
Loc49	Keban (Malatya) metamorphics	38°49′5.70″N,	38°43′39.50″E
Loc53	Guleman (or Maden) volcanics	38°27′47.20″N	39°36′42.00″E
Loc59	Metabasic sample/Pütürge thrust front	38°13′9.70″N	39°12′44.20″E

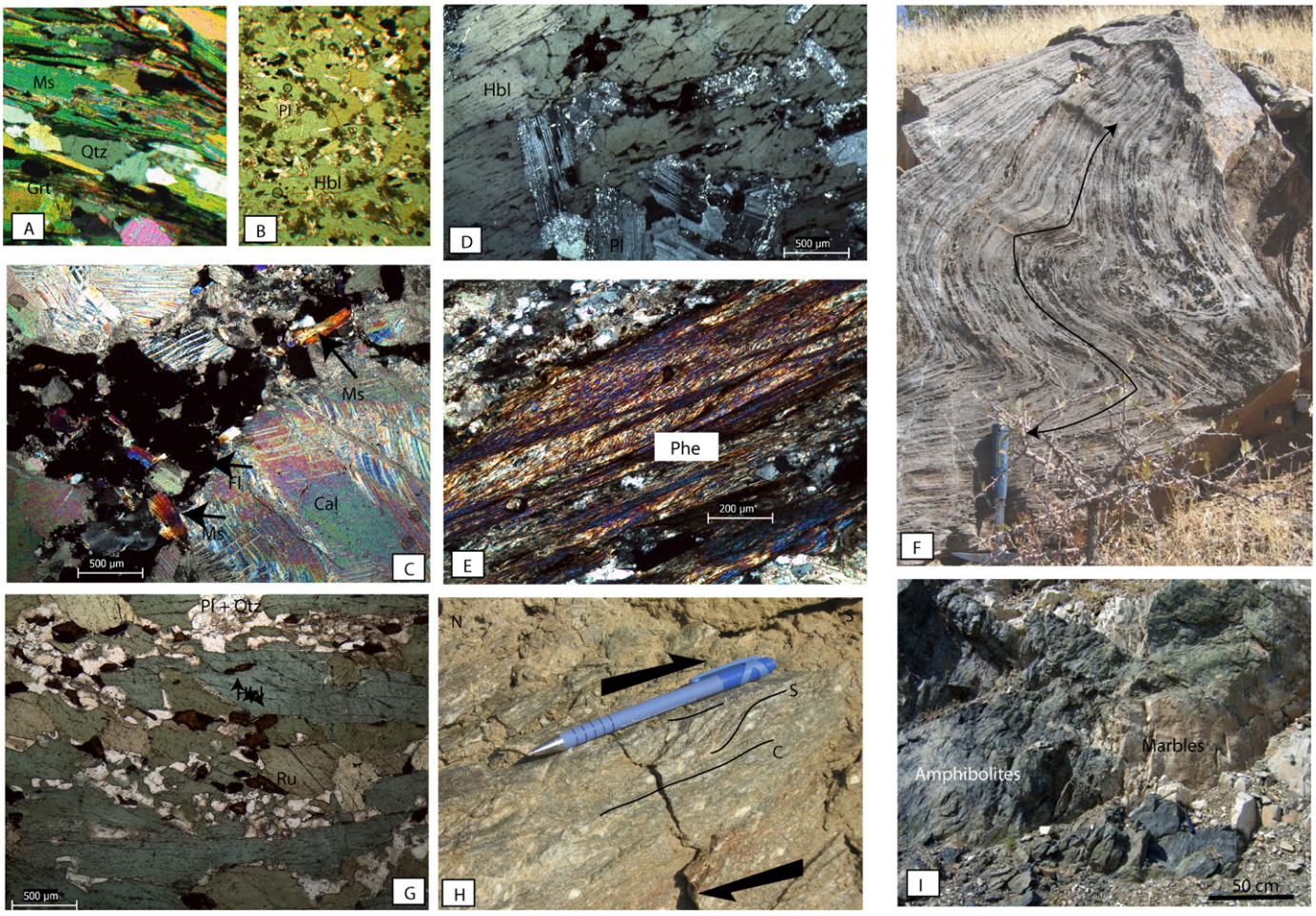

Fig. 6. Field and microphotographs of dated samples. (A) Micaschists (AR-07-07) and B, amphibolite (sample AR-07-08) sampled within a large (~10 m size) block in the N Armenian Upper Cretaceous flysch (location in Fig. 3), for details see Rolland et al. (2011). (C) Metamorphosed fluorite-bearing white marble layer (sample location 49 in Fig. 4) in the Keban-Malatya metamorphic complex (SE Turkey). (D) Gabbro sample (sample location 46 in Fig. 4) sampled at the base of Maden magmatic unit. (E and F) Pütürge micaschists (sample location 28 in Fig. 4) and calc-schists are featured by tight folding and thin white-mica crystallization. (G) Amphibolites from frontal metamorphic sole at the base of the Pütürge unit (sample location 59 in Fig. 4). (H) Gneiss showing S-C fabrics with top-south sense of shear, directly above Loc 59 amphibolites. (I) Field relationships showing amphibolites tightly folded with marbles at the base of the Pütürge unit (location 59 in Fig. 4).

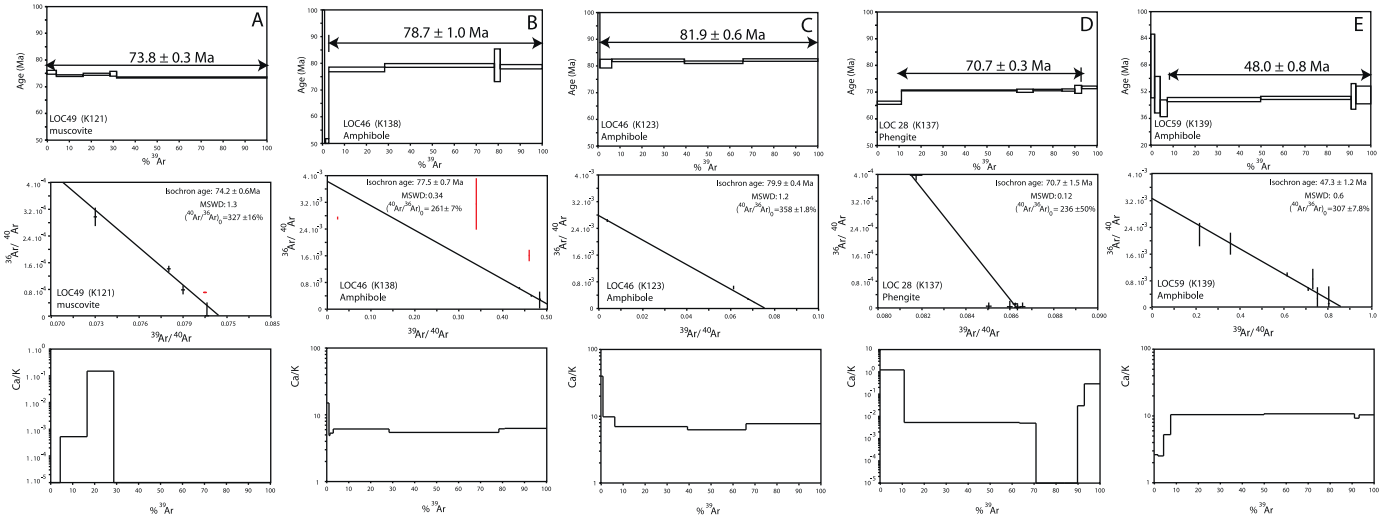

Fig. 7. $^{40}Ar/^{39}Ar$ age spectra of dated SE Turkey samples. (A) Dating of sample Loc49, fluorite-bearing marble of Keban-Malatya unit. (B and C) Datings of amphiboles from sample Loc46, a gabbro of Maden Unit. (D) Dating of phengite from Pütürge metamorphic schists (Loc28). (E) Dating of the basal amphibolite facies shear zone of Pütürge metamorphic unit (sample Loc59).

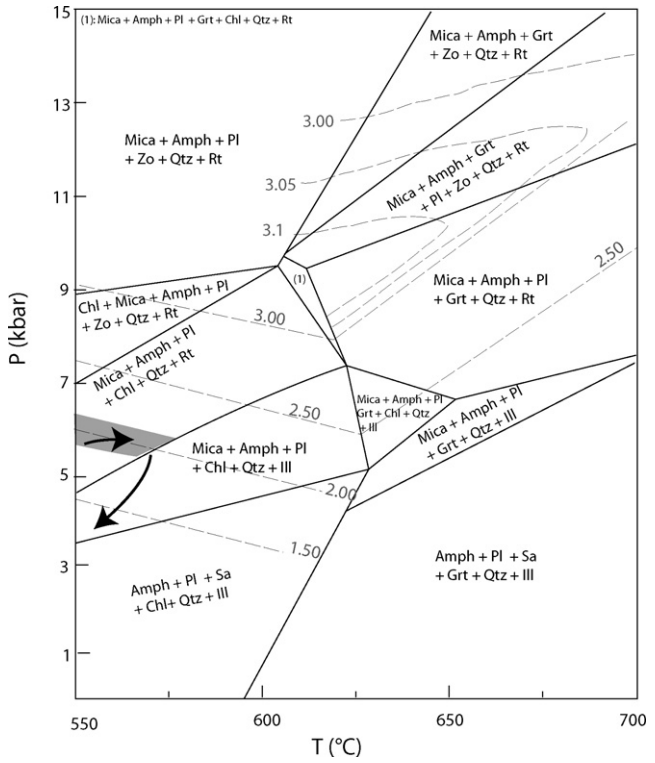

Fig. 8. *P–T* path of amphibolites exposed along the hanging-wall of lower Pütürge unit. Thermobarometry performed on amphibolite sample (location 59 in Fig. 4) was undertaken using PeRpLeX software computed with amphibolite major element composition (Connoly, 1990). Mineral abbreviations are after Kretz (1983).

Upper Jurassic at the same time as the formation of the volcanic arc emplaced onto the Georgian active margin of Eurasia, (2) emplacement of intra-oceanic OIB-type seamounts at c. 117 Ma and (3) obduction of the ophiolite + OIB sequence onto the Armenian block at c. 85–90 Ma (Rolland et al., 2009b). Timing of blueschist and collisional metamorphism in the Stepanavan area are constrained at 90–100 Ma and 71–73 Ma, respectively. In Armenia, the ophiolite obduction and block-Eurasian margin suture were further sealed by Upper Cretaceous to Lower Paleocene pelagic limestone sequences showing that most tectonic displacements had ceased since that time. This ~85–80 Ma age range for the termination of HP metamorphism and ophiolite obduction onto the ATA block(s) in the north coincide with that of (1) emplacement of the tholeiitic Maden volcanic arc in SE Turkey at c. 79–80 Ma, and (2) further active margin magmatism and HT metamorphism evidenced in the southern (Malatya) margin at 74 Ma. Therefore, subduction initiates at the southern rim of the ATA continental block(s) while its northern margin docks into the Northern subduction zone. This temporal relationship supports the idea of a subduction jump from the north to the south of the ATA block(s) in the Campanian at c. 80 Ma.

5.3. Docking of the Bitlis–Pütürge microblock

The HP evolution of the Bitlis–Pütürge is bracketed at 74–71 Ma (Göncüoğlu and Turhan, 1984; Hempton, 1985; Oberhänsli et al., 2010; this study). This metamorphic age is in agreement with a continental subduction event that occurred a long time before the final closure of the southern Neotethys and Arabia–Eurasia collision, suggesting that the Bitlis–Pütürge was a microblock accreted to the ATA continental margin following rapid continental subduction and exhumation of the leading edge of the block. Ar–Ar dates agree for initial subduction of the Eastern Bitlis at 74 Ma followed by underthrusting of the Pütürge blueschists at 71 Ma.

5.4. Subduction of the Southern Neo-Tethys and Arabia–Eurasia collision

The age of Arabia–Eurasia collision itself is still debated as estimates range from Upper Cretaceous (Hall, 1976; Berberian and King, 1981; Alavi, 1994) to late Eocene–Oligocene (40–25 Ma;

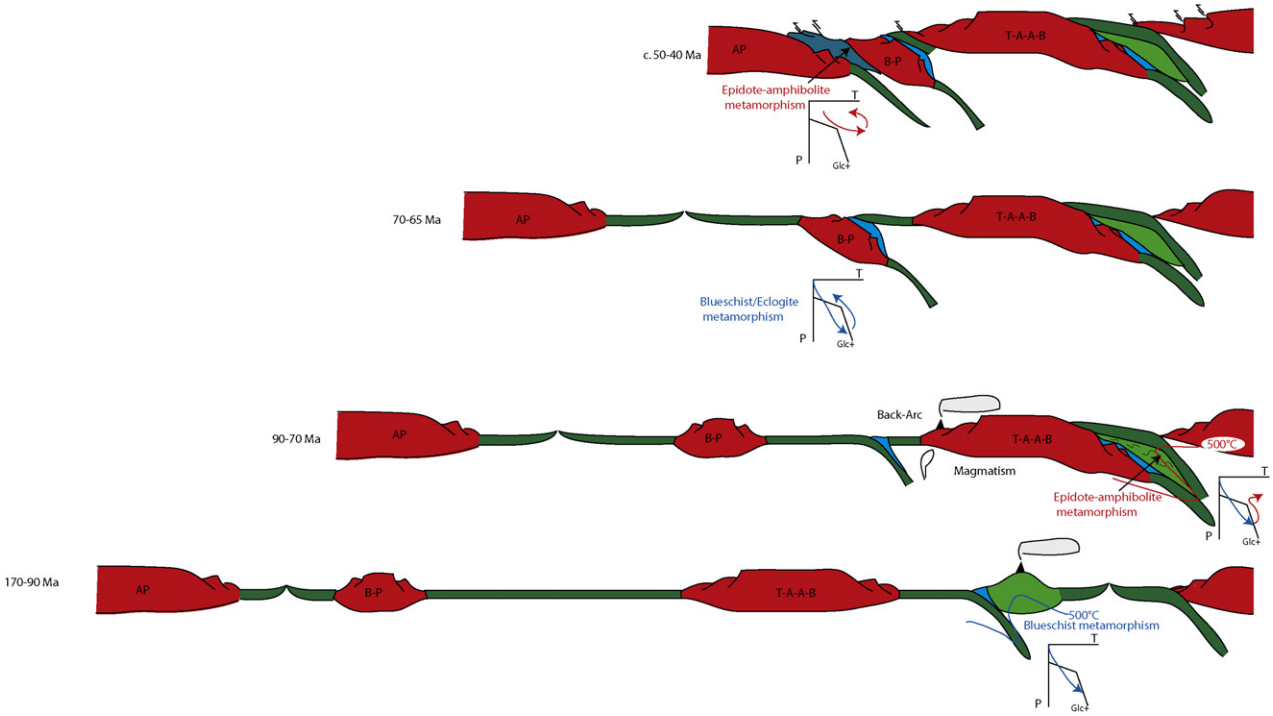

Fig. 9. Simplified evolutionary geodynamic scenario proposed for the Lesser Caucasus–East Anatolia–Arabian Plate transect. Positions of main plate boundaries are according to Barrier and Vrielynck (2008).

Jolivet and Facenna, 2000; Agard et al., 2005; Allen and Armstrong, 2008) and even Miocene (Şengör et al., 1985; Dewey et al., 1986; Okay et al., 2010). These estimates are constrained by stratigraphy and age of deformation in both Arabian and Eurasian plates. But, the history of Arabia–Eurasia collision is complex due to accretion of several blocks along Eurasia and subsequent complex geometries. The final closure of remnant oceanic and back-arc basins, and syn-collisional foreland basins, was highly partitioned and incremental through time. Following the suturing of the Bitlis–Pütürge, the southern Neotethys ocean was subducted below it since c. 70 Ma, and its final closure is witnessed by HT (amphibolite grade) metamorphism at the base of the Pütürge unit, dated at 47 Ma (this study). Thermobarometry performed on sample Loc 59 agrees for burial of metabasalts/metagabbros at 6.0 ± 0.5 kbar and $550 \pm 25\,^{\circ}C$ (Fig. 8) in a hot geothermal gradient of $\sim 23\,^{\circ}C\,km^{-1}$. This geotherm is twice hotter than in a standard subduction, and is more in agreement with a classical collisional Barrovian gradient. Such collisional context is also suggested by the position of the amphibolites on the hanging-wall side of the main frontal thrust transporting the Bitlis–Pütürge units over the Arabian foreland (Fig. 4). It is thus probable that the 48 Ma age of amphibolite metamorphism is related to the insight of Eurasia–Arabia collision, resulting in the underthrusting of Arabia below the Bitlis–Pütürge units (Fig. 9). This possible initial date for collision agrees with stress propagation and fold and thrust belt initiation documented inside the Arabian Plate in the Late Eocene times (Kaymakci et al., 2010). Initiation of extension in the Agean domain (Jolivet and Facenna, 2000) is ascribed to slab retreat initiated in the Oligocene. Slab rollback is suggested for the opening of the Black Sea (Stephenson and Schellart, 2010) following the Arabia–Eurasia collision. As for the Himalayan collision, lateral escape motions are evidenced by the activation of strike-slip faults that initiated some 10–20 Ma after initial collision (e.g., Rolland et al., 2009d). It is therefore logical that lateral extrusion of the Tauride–Anatolide and initiation of Agean slab retreat initiated after the collision of Arabia with the ATA block(s) as is modelled by Faccenna et al. (2006). Further activation of the Dead Sea left lateral fault at c. 20 Ma coincides with acceleration of exhumation documented in the Bitlis thrust zone (Okay et al., 2010). We propose that this acceleration may be tied up to Arabian Plate northward movement related to the opening of the Red Sea rift and further oceanization. In the Late Miocene, activation of North and South Anatolian Faults (e.g., Faccenna et al., 2006) and reorganization of the stress field in Turkey and Armenia (Avagyan et al., 2005, 2010; Kaymakci et al., 2010) agree with northward propagation of strike-slip faulting across the collisional system.

6. Conclusion

Geological investigation and $^{40}Ar/^{39}Ar$ dating undertaken on the main tectonic boundaries of the Anatolide–Tauride–Armenian (ATA) block in Eastern Turkey, Armenia and Georgia provide temporal constraints of subduction and accretion on both sides of this small continental block, and final collisional history of Eurasian and Arabian plates. On the northern side, $^{40}Ar/^{39}Ar$ ages give insights for the subduction and collage from the Middle to Upper Cretaceous (95–80 Ma). To the south, younger magmatic and metamorphic ages exhibit subduction of Neotethys and accretion of the Bitlis–Pütürge block during the Upper Cretaceous (74–71 Ma). These data are interpreted as a subduction jump from the northern to the southern boundary of the ATA continental block at 80–75 Ma. Similar back-arc type geochemistry of obducted ophiolites in the two subduction–accretion domains point to a similar intra-oceanic evolution prior to accretion, featured by slab steepening and rollback as for the current Mediterranean domain. Final closure of Neotethys and initiation of collision with Arabian Plate is suggested to lie in the Middle-Upper Eocene as featured by c. 48 Ma amphibolite facies rocks exhumed in the hanging-wall part of a top-to-the-south thrust at the southern boundary of the Bitlis–Pütürge unit.

Acknowledgements

This study was funded by MEBE and DARIUS grants. The authors wish to thank the reviewer comments of K. Schulman and I. Spalla, which helped increase the scientific value of this paper. This work benefited from discussions held at the International Symposium on the Geology of the Black Sea Region in Ankara (2009). The technical help of M. Manetti in the sample preparation and mineral analysis is also acknowledged.

References

Adamia, S.A., Chkhotua, T., Kekelia, M., Lordkipanidze, M., et al., 1981. Tectonics of the Caucasus and adjoining regions: implications for the evolution of the Tethys ocean. Journal of Structural Geology 3, 437–447.

Agard, P., Omrani, J., Jolivet, L., Mouthereau, F., 2005. Convergence history across Zagros (Iran): constraints from collisional and earlier deformation. International Journal of Earth Sciences 94, 401–419.

Alavi, M., 1994. Tectonics of the Zagros orogenic belt of Iran-New data and interpretations. Tectonophysics 229, 211–238.

Allen, M., Armstrong, H.A., 2008. Arabia–Eurasia collision and the forcing of mid-Cenozoic global cooling. Paleogeography, Paleoclimatology, Paleoecology 265, 52–58.

Avagyan, A., Sosson, M., Philip, M.H., Karakhanian, A., Rolland, Y., Melkonyan, R., Rebai, S., Davtyan, V., 2005. Neogene to quaternary stress field evolution in Lesser Caucasus and adjacent regions using fault kinematics analysis and volcanic cluster data. Geodinamica Acta 18, 401–416.

Avagyan, A., Sosson, M., Karakhanian, A., Philip, H., Rebai, S., Rolland, Y., Melkonyan, R., Davtyan, V., 2010. Recent Ectonic Stress Evolution in the Lesser Caucasus and Adjacent Regions, vol. 340. Geological Society London Special Publications, pp. 393–408.

Barrier, E., Vrielynck, B., 2008. Palaeotectonic Maps of the Middle East Tectono-sedimentary-palinspastic Maps from Late Norian to Piacenzia. Commission for the Geological Map of the World (CGMW/CCGM)/UNESCO, http://www.ccgm.org, Atlas of 14 maps, scale 1/18,500,000.

Berberian, M., King, G., 1981. Toward a paleogeography and tectonic evolution of Iran. Canadian Journal of Earth Sciences 18, 210–265.

Cabanis, M., Lecolle, M., 1989. Le diagramme La/10-Y/15-Nb/8: un outil pour la discrimination des series volcaniques et la mise en évidence des processus de mélange et/ou de contamination crustale. Comptes Rendus De L Academie Des Sciences Serie II 309, 2023–2029.

Connoly, J.A.D., 1990. Calculation of multivariable phase diagrams: an algorithm based on generalized thermodynamics. American Journal of Science 290, 666–718.

Danelian, T., Asatryan, G., Sosson, M., Person, A., Sahakhyan, L., Galoyan, G., 2008. Discovery of Middle Jurassic (Bajocian) Radiolaria from the sedimentary cover of the Vedi ophiolite (Lesser Caucasus, Armenia). Comptes Rendus Palevol 7, 327–334.

Dewey, J.F., Hempton, M.R., Kidd, W.S.F., Saroglu, F., Şengör, A.M.C., 1986. Shortening of continental Lithosphere: the neotectonics of Eastern Anatolia-A young collision zone. In: Coward, M.P., Ries, A.C. (Eds.), Collision Tectonics, vol. 19. Geological Society of London Special Publication, pp. 3–36.

Faccenna, C., Bellier, O., Martinod, J., Piromallo, C., Regard, V., 2006. Slab detachment beneath eastern Anatolia: a possible cause for the formation of the Anatolian Fault. Earth and Planetary Science Letters 242, 85–97.

Floyd, P.A., Goncuoğlu, M.C., Winchester, J.A., Yalınız, M.K., 2000. Geochemical Character and Tectonic Environment of Neotethyan Ophiolitic Fragments and Metabasites in the Central Anatolian Crystalline Complex, Turkey, vol. 173. Geological Society London Special Publication, pp. 183–202.

Galoyan, G., Rolland, Y., Sosson, M., Corsini, M., Melkonyan, R., 2007. Evidence for superposed MORB, oceanic plateau and volcanic arc series in the Lesser Caucasus (Stepanavan, Armenia). Comptes Rendus Geoscience 339, 482–492.

Galoyan, G., Rolland, Y., Sosson, M., Corsini, M., Billo, S., Verati, C., Melkonyan, R., 2009. Geology, geochemistry and $^{40}Ar/^{39}Ar$ dating of Sevan ophiolites (Lesser Caucasus, Armenia): evidence for Jurassic Back-arc opening and hot spot event between the South Armenian Block and Eurasia. Journal of Asian Earth Sciences 34, 135–153.

Göncüoğlu, M.C., Turhan, N., 1984. Geology of the Bitlis Metamorphic Belt. In: Tekeli, O., Göncüoglu, M.C. (Eds.), International Symposium on the Geology of the Taurus Belt, Proceedings. , pp. 237–244.

Hall, R., 1976. Ophiolite emplacement and the evolution of the Taurus suture zone, southeastern Turkey. Geological Society of America Bulletin 87, 1078–1088.

Hempton, M.R., 1985. Structure and deformation history of the Bitlis Suture near Lake Hazar, SE Turkey. Geological Society of America Bulletin 96, 223–243.

Hüsing, S.K., Zachariasse, W.J., Van Hinsbergen, D.J.J., Krijgsman, W., Inceöz, M., Harzhauser, M., Mandic, O., Kroh, A., 2009. Oligo-Miocene foreland basin evolution in SE Anatolia: implications for the closure of the eastern Tethys gateway. In: Van Hinsbergen, D.J.J., Edwards, M.A., Govers, R. (Eds.), Geodynamics of Collision and Collapse at the Africa–Arabia–Eurasia Subduction Zone, vol. 311. Geological Society of London Special Publication, pp. 107–132.

Jolivet, L., Facenna, C., 2000. Mediterranean extension and the Africa–Eurasia collision. Tectonics 19, 1095–1106.

Jourdan, F., Vérati, C., Féraud, G., 2006. Intercalibration of the Hb3gr $^{40}Ar/^{39}Ar$ dating standard. Chemical Geology 231, 177–189.

Kretz, R., 1983. Symbols for rock-forming minerals. American Mineralogist 68, 277–279.

Kaymakci, N., Özcelik, Y., White, S.H., Van Dijk, P.M., 2009. Tectono-stratigraphy of the Çankiri Bas: Late Cretaceous to early Miocene evolution of the Neotethyan Suture Zone in Turkey. In: Van Hinsbergen, D.J.J., Edwards, M.A., Govers, R. (Eds.), Geodynamics of Collision and Collapse at the Africa–Arabia–Eurasia Subduction Zone, vol. 311. Geological Society London Special Publication, pp. 67–106.

Kaymakci, N., Inceöz, M., Ertepinar, P., Koö, A., 2010. Late Cretaceous to recent kinematics of SE Anatolia (Turkey). In: Sosson, M., Kaymakci, N., Stephanson, R., Bergarat, F., Storatchenoko, v. (Eds.), Sedimentary Basin Tectonics from the Black Sea and Caucasus to the Arabian Platform, vol. 340. Geological Society London Special Publication, pp. 409–435.

Kuscu, I., Gencalioglu-Kuscu, G., Tosdal, R.M., Ulrich, T.D., Friedman, R., 2010. Magmatism in the southeastern Anatolian orogenic belt: transition from arc to post-collisional setting in an evolving orogen. In: Sosson, M., Kaymakci, N., Stephanson, R., Bergarat, F., Storatchenoko, V. (Eds.), Sedimentary Basin Tectonics from the Black Sea and Caucasus to the Arabian Platform, vol. 340. Geological Society of London Special Publication, pp. 437–460.

Lordkipanidze, M.B., Meliksetian, B., Djarbashian, R., 1989. Mesozoic–Cenozoic magmatic evolution of the Pontian–Crimean–Caucasian region. In: Rakus, M., Dercourt, J., Nairn, A.E.M. (Eds.), Evolution of the Northern Margin of Tethys: The Results of IGCP 198, vol. 4. Occasional Publications ESRI, New Series, pp. 103–131.

Lytwyn, J.N., Casey, J.F., 1993. The geochemistry and petrogenesis of volcanics and sheeted dikes from the Hatay (Kızıldağ) ophiolite, southern Turkey: possible formation with the Troodos ophiolite, Cyprus, along fore-arc spreading centers. Tectonophysics 232, 237–272.

Oberhänsli, R., Candan, O., Bousquet, R., Rimmele, G., Okay, A., Goff, J., 2010. Alpine HP evolution of the eastern Bitlis complex, SE Turkey. In: Sosson, M., Kaymakci, N., Stephanson, R., Bergarat, F., Storatchenoko, V. (Eds.), Sedimentary Basin Tectonics from the Black Sea and Caucasus to the Arabian Platform, vol. 340. Geological Society of London Special Publication, pp. 461–483.

Okay, A.I., Tüysüz, O., Satır, M., Özkan-Altıner, S., Altıner, D., Sherlock, S., Eren, R.H., 2006. Cretaceous and Triassic subduction-accretion, HP/LT metamorphism and continental growth in the Central Pontides, Turkey. GSA Bulletin 118, 1247–1269, doi:10.1130/B25938.1.

Okay, A.I., Zattin, M., Cavazza, W., 2010. Apatite fission-track data for the Miocene Arabia–Eurasia collision. Geology 38, 35–43, doi:10.1130/G30234.

Parlak, O., Delaloye, M., Bingöl, E., 1996. Mineral chemistry of ultramafic and mafic cumulates as an indicator of the arc-related origin of the Mersin ophiolite (southern Turkey). Geologische Rundschau 85, 647–661.

Parlak, O., Höck, V., Delaloye, M., 2000. Suprasubduction Zone Origin of the Pozanti-Karsanti Ophiolite (southern Turkey) deduced from Whole-Rock and Mineral Chemistry of the Gabbroic Cumulates, vol. 173. Geological Society London Special Publication, pp. 219–234.

Parlak, O., Rızaoğlu, T., Bağcı, U., Karaoğlan, F., Höck, V., 2009. Tectonic significance of the geochemistry and petrology of ophiolites in southeast Anatolia, Turkey. Tectonophysics 473, 173–187.

Perinçek, D., Özkaya, İ., 1981. Tectonic evolution of the northern margin of Arabian Plate. Bulletin of Earth Sciences of Hacettepe University, Ankara 8, 91–101.

Ricou, L.E., Dercourt, J., Geyssant, J., Grandjacquet, C., Lepvrier, C., Biju-Duval, B., 1986. Geological constraints on the Alpine evolution of the Mediterranean Tethys. Tectonophysics 123, 83–122.

Robertson, A.H.F., 2002. Overview of the genesis and emplacement of Mesozoic ophiolites in the Eastern Mediterranean Tethyan region. Lithos 65, 1–67.

Rolland, Y., Billo, S., Corsini, M., Sosson, M., Galoyan, G., 2009a. Blueschists of the Amassia–Stepanavan Suture Zone (Armenia): linking Tethys subduction history from E-Turkey to W-Iran. International Journal of Earth Science 98, 533–550, doi:10.1007/s00531-007-0286-8.

Rolland, Y., Galoyan, G., Bosch, D., Sosson, M., Corsini, M., Fornari, M., Vérati, C., 2009b. Jurassic Back-arc and hot-spot related series in the Armenian ophiolites – implications for the obduction process. Lithos 112, 163–187, doi:10.1016//j.lithos.2009.02.006.

Rolland, Y., Cox, S.F., Corsini, M., 2009c. Constraining deformation stages in brittle-ductile shear zones from combined field mapping and $^{40}Ar/^{39}Ar$ dating: the structural evolution of the Grimsel Pass area (Aar massif, Swiss Alps). Journal of Structural Geology 31, 1377–1394, doi:10.1016/j.jsg.2009.08.003.

Rolland, Y., Mahéo, G., Pêcher, A., Villa, I.M., 2009d. Syn-kinematic emplacement of the Pangong metamorphic and magmatic complex along the Karakorum Fault (N Ladakh). Journal of Asian Earth Sciences 34, 10–25.

Rolland, Y., Galoyan, G., Sosson, M., Melkonian, R., Avagyan, A., 2010. The Armenian ophiolites: insights for Jurassic Back-arc formation, lower Cretaceous hot-spot magmatism and upper Cretaceous obduction over the South Armenian Block. In: Sosson, M., Kaymakci, N., Stephanson, R., Bergarat, F., Storatchenoko, V. (Eds.), Sedimentary Basin Tectonics from the Black Sea and Caucasus to the Arabian Platform, vol. 340. Geological Society of London Special Publication, pp. 353–382.

Rolland, Y., Sosson, M., Adamia, S., Sadradze, N., 2011. Prolonged Variscan to Alpine history of an active Eurasian margin (Georgia Armenia) revealed by $^{40}Ar/^{39}Ar$ dating. Gondwana Research 20, 798–815, doi:10.1016/j.gr.2011.05.007.

Rolland, Y., Lardeaux, J.-M., Jolivet, L., 2012. Deciphering orogenic evolution. Journal of Geodynamics 56-57, 1–6.

Şengör, A.M.C., Görür, N., Saroglu, F., 1985. Strike-slip faulting and related basin formation in zones of tectonic escape: Turkey as a case study. In: Biddle, K.D., Christie-Blick, N. (Eds.), Strike-slip Deformation, Basin formation and Sedimentation, vol. 17. Society of Economic Paleontologists and Mineralogists Special Publication, pp. 227–264.

Sosson, M., Rolland, Y., Danelian, T., Muller, C., Melkonyan, R., Adamia, S., Kangarli, T., Avagyan, A., Galoyan, G., 2010. Subductions, obduction and collision in the Lesser Caucasus (Armenia Azerbaijan, Georgia), new insights. In: Sosson, M., Kaymakci, N., Stephanson, R., Bergarat, F., Storatchenoko, V. (Eds.), Sedimentary Basin Tectonics from the Black Sea and Caucasus to the Arabian Platform, vol. 340. Geological Society of London Special Publication, pp. 329–352.

Stephenson, R., Schellart, W.P., 2010. The Black Sea back-arc basin: insights to its origin from geodynamic models of modern analogues. In: Sosson, M., Kaymakci, N., Stephanson, R., Bergarat, F., Storatchenoko, V. (Eds.), Sedimentary Basin Tectonics from the Black Sea and Caucasus to the Arabian Platform, vol. 340. Geological Society of London Special Publication, pp. 11–21.

Vanderhaeghe, O., 2012. The thermal–mechanical evolution of Crustal Orogenic belts at convergent plate boundaries: a reappraisal of the orogenic cycle. Journal of Geodynamics 56–57, 124–145.

Vincent, S.J., Allen, M.B., Ismail-Zadeh, A.D., Flecker, R., Foland, K.A., Simmons, M.D., 2005. Insights from the Talysh of Azerbaijan into the Paleogene evolution of the South Caspian region. Geological Society of America Bulletin 117, 1513–1533.

Yalınız, K.M., Floyd, P., Goncuoğlu, M.C., 1996. Supra-subduction zone ophiolites of Central Anatolia: geochemical evidence from the Sarikaraman ophiolite, Aksaray, Turkey. Mineralogical Magazine 60, 697–710.

Yılmaz, Y., 1993. New evidence and model on the evolution of the southeast Anatolian orogen. Geological Society of America Bulletin 105, 251–271.